

KINETICS, CATALYSIS, AND REACTION ENGINEERING

Kinetic Model for the Etherification of 2,4,4-Trimethyl-1-pentene and 2,4,4-Trimethyl-2-pentene with Methanol

Reetta S. Karinen* and A. Outi I. Krause

Laboratory of Industrial Chemistry, Helsinki University of Technology, P.O. Box 6100, FIN-02015 HUT, Finland

Etherification of 2,4,4-trimethyl-1-pentene and 2,4,4-trimethyl-2-pentene with methanol was catalyzed with a novel Smopex-101 catalyst, which is a polyethylene-based ion-exchange fiber. Several kinetic models were tested to describe the experimental data. The Langmuir-Hinshelwood-type model, in which the adsorption of alkenes is assumed to be weak relative to methanol and ether, described the data well. The activation energies obtained for the etherification of 2,4,4-trimethyl-1-pentene and 2,4,4-trimethyl-2-pentene were 86 ± 1 and 80 ± 2 kJ/mol, respectively. These values are on the same level as those typically found for similar etherification reactions. An equally good fit was obtained with the Eley-Rideal-type model, which assumes that the alkenes react without adsorption. In both models the adsorption constants for methanol and ether are of the same order of magnitude. This constitutes a significant difference from the modeling results obtained with conventional ion-exchange resin catalysts and can be explained by the nature of the polymer matrixes.

Introduction

Ethers have been used in gasoline as octane boosters for a few decades now. Recently, however, methyl-*tert*-butyl ether (MTBE; 2-methoxy-2-methylpropane), the most widely used ether, was detected in groundwater. Therefore, the world's major consumer of MTBE, the state of California, has banned its use after the end of 2002.¹

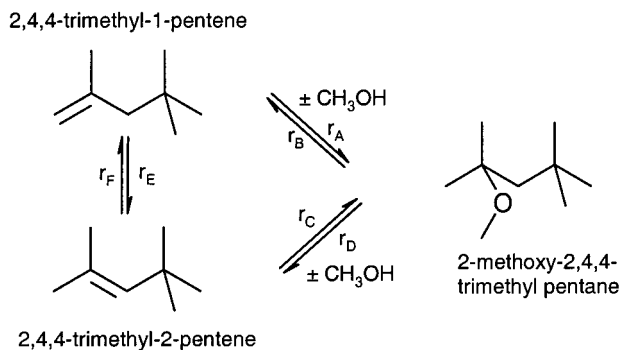
Refineries in the U.S.A. and Canada are seeking new applications for the existing MTBE plants and isobutene feedstock. Some companies have already announced new process configurations to produce high-octane gasoline components from isobutene in the present MTBE plants.²⁻⁴ In these processes isobutene is first dimerized to isooctenes, which are then hydrogenated to isooctane (2,2,4-trimethylpentane). With its high octane rating, the dimeric stream itself is suitable for the gasoline pool,⁵ as long as the upper limits for the olefin (alkene) content are not exceeded.

The main dimeric products of isobutene are 2,4,4-trimethyl-1-pentene (TMP1) and 2,4,4-trimethyl-2-pentene (TMP2). These components have a double bond at a tertiary carbon, which makes them reactive in etherification.⁶ The resulting ether, 2-methoxy-2,4,4-trimethylpentane, is reported to have a high octane rating with a blending octane number of 147.⁷ Although it has recently been shown that the blending octane numbers are 99 (BMON) and 110 (BRON),⁸ the octane rating is still on the same level as those of commercially produced ethers.⁹ Introduction of oxygen to the gasoline pool via this ether is thus feasible. The presence of oxygen in

fuel improves the combustion and reduces the emissions of unburned hydrocarbons and carbon monoxide. Furthermore, ethers with higher molecular mass have lower vapor pressure and higher boiling point,⁹ which is advantageous for gasoline blending. They are also less soluble in water,⁹ and the problems encountered with MTBE are not expected.

The kinetics of etherification of C₄-C₆ alkenes has been studied relatively widely, and the mechanisms generally proposed for the reactions are of Eley-Rideal type [e.g., for MTBE,¹⁰ for ethyl *tert*-butyl ether (ETBE),¹¹ for *tert*-amyl methyl ether (TAME),¹²⁻¹⁴ and for *tert*-amyl ethyl ether (TAEE)¹⁵] and of Langmuir-Hinshelwood type [e.g., for ETBE,¹⁶ for TAME,¹⁷ for TAEE,¹⁸ and for *tert*-hexyl ethyl ether (THEE)¹⁹] reaction mechanisms. The kinetics of the etherification of C₈ alkenes, in turn, has not been studied. As the carbon number of the alkene participating in the reaction increases, the reaction rate slows down and the equilibrium conversion decreases,²⁰ and therefore the etherification reaction of the C₈ alkenes is relatively slow compared with that of commercially produced ethers.^{6,21} New catalysts have been tested to enhance the reaction rate, and lately we have found that, in the etherification reaction of C₈ alkenes, a novel fibrous catalyst is more active than the traditional ion-exchange resin beads.²² In this work we derive a kinetic model for the etherification reaction of 2,4,4-trimethylpentenes with methanol where the catalyst is not an ion-exchange resin, as is usually the case, but a novel Smopex-101 ion-exchange fiber. Although the reaction rate is slow with the 2,4,4-trimethylpentenes of the study, the industrial interest and commercial potential of these alkenes²⁻⁴ make our study important.

* Corresponding author. Fax: +358-9-451 2622. E-mail: reetta.karinen@hut.fi.

Scheme 1. Reaction Scheme for the Etherification of 2,4,4-Trimethylpentenes with Methanol

Experimental Section

Reactor. The experiments were carried out in an 80 cm³ stainless steel batch reactor equipped with a magnetic stirrer (stirring speed 1000 rpm) and a mixing baffle. The reactor was placed in a water bath, through which the temperature of the reactor (60–90 °C) was adjusted. The reaction pressure was maintained at 0.8 MPa with nitrogen to ensure that the reaction mixture remained in the liquid phase. Liquid samples were taken from the reaction mixture manually via a sample valve by overpressurizing the reactor. In a typical experiment, samples were taken at reaction times of 20, 40, 60, 90, 120, 240, and 360 min.

Chemicals. The reactants were methanol (Riedel de Haën, 99.8%), a mixture of 2,4,4-trimethyl-1-pentene and 2,4,4-trimethyl-2-pentene (diisobutylene; Fluka Chemica AG, 95%), 2,4,4-trimethyl-1-pentene (Fluka Chemica AG, >98%), and 2,4,4-trimethyl-2-pentene (Fluka Chemica AG, >98%). The ether, 2-methoxy-2,4,4-trimethylpentane (>98%), was synthesized by Fortum Oil and Gas Oy. Isooctane (2,2,4-trimethylpentane; Merck, >99.5%) was used as an inert solvent, and nitrogen (Aga, 99.5%) was used for pressurization of the reactor.

Catalyst. The catalyst was Smopex-101 (Smoptech Ltd.), a polyethylene-based ion-exchange fiber prepared by grafting a polyethylene fiber with styrene and then sulfonating the grafted fiber with chlorosulfonic acid. The acid capacity of the fiber was 3.75 mmol/g_{cat}, the length 0.25 mm, and the diameter 30 μm. Before the experiment the catalyst was washed with ethanol and dried to remove moisture and other possible impurities. Water must be removed as completely as possible before the reaction because it readily reacts with alkenes to form tertiary alcohol. In addition to accelerating the undesired side reactions, water also inhibits the etherification reaction and decreases the selectivity toward ether.^{23,24} Approximately 0.7 g of Smopex-101 was placed in the reactor as a slurry.

Analytical Methods. Samples were analyzed with a Hewlett-Packard 5890 series II gas chromatograph equipped with a capillary column DB-1 (J&W Scientific; length 60 m, film thickness 1.00 μm, diameter 0.250 mm) and a flame ionization detector. The products were quantified by an internal standard method.

Reaction Scheme. The general reaction scheme of the etherification of 2,4,4-trimethylpentenes with methanol is presented in Scheme 1. All of the reactions are equilibrium-limited, and the net rates for the formation of each component are

$$r_{\text{MeOH}} = (-r_A + r_B) + (-r_C + r_D) = -r_1 - r_2 \quad (1)$$

$$r_{\text{TMP1}} = (-r_A + r_B) + (-r_E + r_F) = -r_1 - r_3 \quad (2)$$

$$r_{\text{TMP2}} = (-r_C + r_D) + (r_E - r_F) = -r_2 + r_3 \quad (3)$$

$$r_{\text{eth}} = (r_A - r_B) + (r_C - r_D) = r_1 + r_2 \quad (4)$$

where subscript 1 refers to the etherification of TMP1, subscript 2 the etherification of TMP2, and subscript 3 the isomerization of TMP1 to TMP2.

The equilibrium constants K_i for each reaction were obtained from our previous work,^{25,26} and the equations for the K_i 's were

$$K_1 = K_2 K_3 \quad (5)$$

$$K_2 = \exp\left(-8.74 + \frac{2740.7}{T}\right) \quad (6)$$

$$K_3 = \exp\left(-0.056 - \frac{421.67}{T}\right) \quad (7)$$

Eley–Rideal (ER)-Type Model. In the noncompetitive adsorption model, an ER-type model, a molecule adsorbed on the catalyst reacts with a molecule from the bulk phase. Here we assume, as is generally proposed for etherification reactions, that methanol is adsorbed on the catalyst and alkenes react from the bulk phase. It is assumed that all of the active surface sites (S) are equal and each component occupies one surface site when adsorbed.



If it is assumed that the surface reaction is the rate-determining step, the reaction rate for the etherification of TMP1 is obtained from eq 8b as

$$r_1 = k_1 \Theta_{\text{MeOH}} a_{\text{TMP1}} - k_{-1} \Theta_{\text{eth}} \quad (9)$$

where Θ_i denotes the surface coverage of component i on the catalyst ($\sum \Theta_i = 1$) and a_i the activity of component i in the bulk phase. In reaction rate equations, the rate constant k_i presents the forward reaction and k_{-i} the backward reaction. The Arrhenius-type equation of the rate constant was rewritten as

$$k = k_{\text{ref}} \exp\left[-\frac{E_{\text{act}}}{R} \left(\frac{1}{T} - \frac{1}{T_{\text{ref}}}\right)\right] \quad (10)$$

where k_{ref} is an average rate constant at the temperature T_{ref} . In the modeling, 80 °C was used as the reference temperature. To enhance the convergence of the parameters, the equation was further reparametrized²⁷ to

$$k = \exp(-P_1) \exp\left[-\exp(P_2) \left(\frac{1}{T} - \frac{1}{T_{\text{ref}}}\right)\right] \quad (11)$$

where P_1 and P_2 are the parameters to be fitted. The same reparametrization was used for the reaction rate constants in all of the modeling.

Here it was assumed that isooctane, which was used as an inert solvent, is not adsorbed on the catalyst, because the adsorption of nonpolar saturated hydrocarbons on ion-exchange resin is minor.²⁸ The surface coverages of MeOH and ether are solved from eq 8a,c. Because these are not the rate-determining steps, the rate is set to zero and the adsorption constants are

$$K_i = \Theta_i / a_i \Theta_S \quad (12)$$

The surface coverages of MeOH and ether obtained from eq 12 are inserted into the reaction rate equation (9) to obtain

$$r_1 = \frac{k_1 K_{\text{MeOH}} a_{\text{MeOH}} a_{\text{TMP1}} - k_{-1} K_{\text{eth}} a_{\text{eth}}}{1 + K_{\text{MeOH}} a_{\text{MeOH}} + K_{\text{eth}} a_{\text{eth}}} \quad (13)$$

The first term in the denominator of eq 13 is assumed to be small because of the strong adsorption of the polar components on the catalyst,^{13,14,17} and it can be neglected. We also modeled the case where the first term is included in the model, and dropping out the first term of the denominator is discussed also later in the paper. The thermodynamic equilibrium constant of the overall reaction can be expressed as

$$K_1 = \frac{k_1}{k_{-1}} \frac{K_{\text{MeOH}}}{K_{\text{eth}}} \quad (14)$$

When the equilibrium constant is inserted in eq 13 and the equation is rewritten, we obtain

$$r_i = \frac{k_i \left(a_{\text{MeOH}} a_{\text{TMP}i} - \frac{a_{\text{eth}}}{K_i} \right)}{a_{\text{MeOH}} + \frac{K_{\text{eth}}}{K_{\text{MeOH}}} a_{\text{eth}}} \quad i = 1, 2 \quad (15)$$

and the rate equation for the isomerization of TMP1 to TMP2

$$r_3 = k_3 a_{\text{TMP1}} - k_{-3} a_{\text{TMP2}} = k_3 (a_{\text{TMP1}} - a_{\text{TMP2}} / K_3) \quad (16)$$

The adsorption constants are temperature-dependent parameters, and thus also their ratios are temperature-dependent. This was neglected in our models because the temperature dependency of the adsorption is small relative to that of the reaction rate: for example, the adsorption enthalpy for methanol on the ion-exchange resins is reported to be -3.8 kJ/mol,²⁹ whereas activation energies of etherification are typically over 70 or 80 kJ/mol. Also the narrow temperature range (60–90 °C) enables us to neglect the temperature dependency of the adsorption constants and to use constant values instead. Furthermore, when ratios of the adsorption constants are used, the temperature dependencies of the individual constants reduce each other and the temperature dependency of the ratio is smaller than that of the individual constants.

Langmuir–Hinshelwood (LH)-Type Model. In a competitive adsorption model, the LH-type model, all of the components are adsorbed on the catalyst and the adsorbed species react. Also here it is assumed that each component occupies one active site and all sites are equal.



The rate-determining step is assumed to be the surface reaction (17d). The adsorption constants are determined as presented in eq 12. The adsorption constants for TMP1 and TMP2 were assumed to be approximately the same, and the terms were combined. With a procedure similar to that presented with the ER model, we obtain for the etherification of TMP1

$$r_1 = \frac{k_1 K_{\text{MeOH}} K_{\text{TMP}} a_{\text{MeOH}} a_{\text{TMP1}} - k_{-1} K_{\text{eth}} a_{\text{eth}}}{[1 + K_{\text{MeOH}} a_{\text{MeOH}} + K_{\text{TMP}} (a_{\text{TMP1}} + a_{\text{TMP2}}) + K_{\text{eth}} a_{\text{eth}}]^2} \quad (18)$$

Now the equilibrium constant of the overall reaction is

$$K_1 = \frac{k_1}{k_{-1}} \frac{K_{\text{MeOH}} K_{\text{TMP}}}{K_{\text{eth}}} \quad (19)$$

and by inserting and rearranging, as presented with the ER model, we obtain for the etherification of TMP1 and TMP2

$$r_i = \frac{k_i \frac{K_{\text{TMP}}}{K_{\text{MeOH}}} \left(a_{\text{MeOH}} a_{\text{TMP}i} - \frac{a_{\text{eth}}}{K_i} \right)}{\left(a_{\text{MeOH}} + \frac{K_{\text{TMP}}}{K_{\text{MeOH}}} (a_{\text{TMP1}} + a_{\text{TMP2}}) + \frac{K_{\text{eth}}}{K_{\text{MeOH}}} a_{\text{eth}} \right)^2} \quad i = 1, 2 \quad (20)$$

and the rate equation for the isomerization of alkenes is

$$r_3 = \frac{k_3 \frac{K_{\text{TMP}}}{K_{\text{MeOH}}} \left(a_{\text{TMP2}} - \frac{a_{\text{TMP2}}}{K_3} \right)}{a_{\text{MeOH}} + \frac{K_{\text{TMP}}}{K_{\text{MeOH}}} (a_{\text{TMP1}} + a_{\text{TMP2}}) + \frac{K_{\text{eth}}}{K_{\text{MeOH}}} a_{\text{eth}}} \quad (21)$$

Results and Discussion

Data for the Modeling. The experimental data consisted of 43 batch experiments. Some experiments were repeated to test the reliability of the data, but only one experiment for each set of conditions was included in the modeling. All of the experiments were evaluated carefully prior to the modeling, and all of the experiments where the carbon mole balance was less than 95% were rejected. The experiments that were included in the modeling are presented in Table 1, and in these data the carbon mole balance was, on the average, 99%.

The initial etherification rates are presented in Table 1. In the experiments where ether was in the feed the rates refer to the decomposition rate of the ether. Typical alkene conversions, which were achieved within 6 h with a stoichiometric feed of alkene and methanol, were up to 9% with the isomer mixture, 22% with pure TMP1, and 45% with pure TMP2. These figures refer to the highest reaction temperature, 90 °C. The conversions were higher with the pure TMP1 and TMP2 than

Table 1. Experiments for the Modeling

| <i>T</i> /°C | reactant ^a | MeOH/alkene molar ratio | mole fractions in feed | | | | initial etherification rate/[mmol/(s kg _{cat})] |
|--------------|-----------------------|-------------------------|------------------------|--------|-----------|-------|---|
| | | | MeOH | alkene | isooctane | ether | |
| 60 | DIB | 0.2 | 0.1 | 0.5 | 0.4 | | 0.4 |
| 80 | DIB | 0.2 | 0.1 | 0.5 | 0.4 | | 2.3 |
| 60 | DIB | 0.5 | 0.27 | 0.53 | 0.2 | | 0.5 |
| 70 | DIB | 0.5 | 0.27 | 0.53 | 0.2 | | 1.4 |
| 80 | DIB | 0.5 | 0.27 | 0.53 | 0.2 | | 4.1 |
| 90 | DIB | 0.5 | 0.27 | 0.53 | 0.2 | | 8.1 |
| 60 | DIB | 1 | 0.45 | 0.45 | 0.1 | | 0.8 |
| 70 | DIB | 1 | 0.45 | 0.45 | 0.1 | | 1.9 |
| 80 | DIB | 1 | 0.45 | 0.45 | 0.1 | | 4.4 |
| 90 | DIB | 1 | 0.45 | 0.45 | 0.1 | | 10.6 |
| 60 | DIB | 2 | 0.53 | 0.27 | 0.2 | | 0.5 |
| 70 | DIB | 2 | 0.53 | 0.27 | 0.2 | | 1.5 |
| 80 | DIB | 2 | 0.53 | 0.27 | 0.2 | | 3.7 |
| 90 | DIB | 2 | 0.53 | 0.27 | 0.2 | | 7.6 |
| 60 | DIB | 5 | 0.5 | 0.1 | 0.4 | | 0.2 |
| 80 | DIB | 5 | 0.5 | 0.1 | 0.4 | | 1.1 |
| 60 | TMP1 | 1 | 0.15 | 0.15 | 0.7 | | 0.7 |
| 70 | TMP1 | 1 | 0.15 | 0.15 | 0.7 | | 2.0 |
| 80 | TMP1 | 1 | 0.15 | 0.15 | 0.7 | | 4.6 |
| 90 | TMP1 | 1 | 0.15 | 0.15 | 0.7 | | 10.2 |
| 60 | TMP1 | 2 | 0.27 | 0.13 | 0.6 | | 0.5 |
| 80 | TMP1 | 2 | 0.27 | 0.13 | 0.6 | | 3.6 |
| 60 | TMP1 | 0.5 | 0.27 | 0.53 | 0.2 | | 0.5 |
| 80 | TMP1 | 0.5 | 0.27 | 0.53 | 0.2 | | 3.7 |
| 70 | TMP2 | 1 | 0.15 | 0.15 | 0.7 | | 0.5 |
| 80 | TMP2 | 1 | 0.15 | 0.15 | 0.7 | | 1.0 |
| 90 | TMP2 | 1 | 0.15 | 0.15 | 0.7 | | 1.8 |
| 60 | ether | | | | 0.7 | 0.3 | 7.1 ^b |
| 70 | ether | | | | 0.7 | 0.3 | 8.7 ^b |
| 80 | ether | | | | 0.7 | 0.3 | 18.3 ^b |
| 90 | ether | | | | 0.7 | 0.3 | 57.0 ^b |

^a DIB = mixture of 2,4,4-trimethyl-1-pentene and 2,4,4-trimethyl-2-pentene. TMP1 = 2,4,4-trimethyl-1-pentene. TMP2 = 2,4,4-trimethyl-2-pentene. ^b Ether decomposition rate.

with the isomer mixture because, in addition to the etherification, isomerization of alkenes occurs.

In the decomposition of ether, respective conversions of up to 93% were achieved within 6 h, which shows that the decomposition of ether is noticeably faster than the formation. The thermodynamic equilibrium plays a role here: the equilibrium limits the formation reaction in the early stages, and the rate of formation is decreased; the thermodynamic equilibrium is not encountered in as early a stage in the decomposition reaction, and the driving force for the decomposition is higher.

Etherification was the main reaction to occur with pure TMP1 with initial rates 3–6 times as high as for the isomerization reaction. With the TMP2 feed, initially the etherification was the main reaction, but the isomerization soon overtook the etherification. TMP1 is thermodynamically the more stable isomer,²⁵ and thus the driving force for the isomerization of TMP2 to TMP1 is greater than that for the reverse reaction.

The selectivity to the ether was good. Hydration of the alkenes to 2,4,4-trimethyl-2-pentanol was observed as a side reaction, but the conversion remained low. The water required for this reaction originates from the impurities of the reactants and the catalyst. Special attention was accordingly paid to the drying and handling of the catalyst to ensure that it was as dry as possible. In the ether formation experiments, the conversion to 2,4,4-trimethyl-2-pentanol was less than 0.1%, which is less than 2% of the total reacted alkene. The ether contained more water as an impurity than the other feeds, and the maximum conversion to 2,4,4-trimethyl-2-pentanol was 0.75% in the ether decomposition experiments. Traces of another side product, dimethyl

ether, were detected in a few experiments. Dimethyl ether is formed from methanol at higher temperatures, and here it was not detected below 80 °C.

Fitting of the Kinetic Parameters. The kinetic parameters were estimated with Kinf software³⁰ by minimizing the sum of squares of the residuals between the measured and calculated compositions of the reaction mixture. The minimizing was performed by the Levenberg–Marquardt method. Because of the nonideality of the reaction mixture, activities instead of concentrations were used in the rate equations, and the activity coefficients were determined by the UNIFAC method.³¹ The activity coefficient of methanol varied between 1 and 10 and that of alkenes between 1.0 and 2.3.

ER-Type Model. Altogether seven parameters had to be fitted in the ER model. In addition to activation energies and rate constants, the ratio of $K_{\text{eth}}/K_{\text{MeOH}}$ was estimated. It was observed that, as the $K_{\text{eth}}/K_{\text{MeOH}}$ ratio was varied between 2 and 3, the activation energy of the isomerization reaction (E_3) varied between 110 and 121 kJ/mol, while the activation energies of etherification varied only between 88 and 89 kJ/mol (E_1) and between 79 and 82 kJ/mol (E_2). It was assumed that the fitting of the isomerization reaction was sensitive because half of the data was from experiments done with the mixture of alkenes, in which the molar ratio of isomers is close to the thermodynamic equilibrium ratio and isomerization is minimal. Thus, the isomerization was modeled separately with the data from the 15 experiments where the feed was pure TMP1, TMP2, or ether (see Table 1). Now we obtained 99 kJ/mol for the activation energy of the isomerization reaction. This value was then fixed in the further modeling, and the

Table 2. Modeling Results

| | ER model | rearranged ER model | LH model | LH without adsorption term of alkene |
|--------------------------|---------------------|---------------------|---------------------|--------------------------------------|
| E_1 , kJ/mol | 89 ± 1 | 94 ± 1 | 87 ± 1 | 86 ± 1 |
| E_2 , kJ/mol | 81 ± 2 | 90 ± 2 | 83 ± 2 | 80 ± 2 |
| E_3 , kJ/mol | 99 ± 3 | 101 ± 4 | 103 ± 20 | 137 ± 5 |
| $k_{1,ref}$, mol/(kg s) | 0.0064 ± 0.0001 | 0.0058 ± 0.0002 | 0.0518 ± 0.0105 | 0.0065 ± 0.0001 |
| $k_{2,ref}$, mol/(kg s) | 0.0064 ± 0.0001 | 0.0056 ± 0.0002 | 0.0486 ± 0.0101 | 0.0062 ± 0.0001 |
| $k_{3,ref}$, mol/(kg s) | 0.0015 ± 0.0001 | 0.0019 ± 0.0001 | 0.0098 ± 0.0022 | 0.0010 ± 0.0001 |
| K_{eth}/K_{MeOH} | 2.4 ± 0.1 | | 2.8 ± 0.1 | 2.5 ± 0.1 |
| K_{MeOH}/K_{eth} | | 1.1 ± 0.1 | | |
| K_{TMP}/K_{MeOH} | | | 0.14 ± 0.03 | |
| residual sum of squares | 0.00297 | 0.0051 | 0.00333 | 0.00294 |

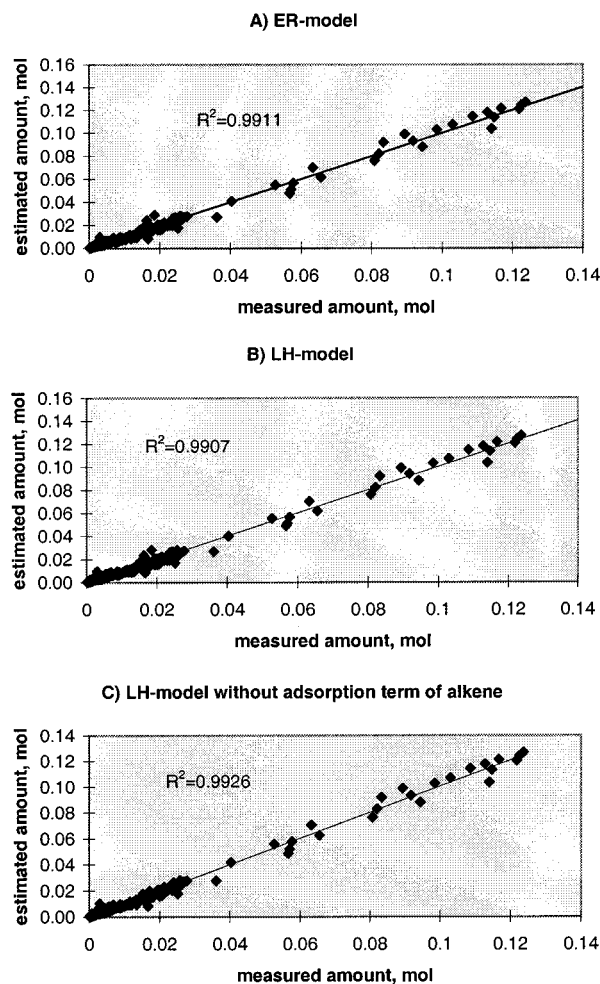


Figure 1. Estimated amount of ether as a function of the measured amount: (A) ER model; (B) LH model; (C) LH model without the adsorption term of alkene.

whole data set of Table 1 was used to model the rest of the parameters. The results of the modeling are collected in Table 2, and Figure 1 presents the estimated amount of ether as a function of the measured amounts. As an example, Figure 2 shows how the ER model interprets the experimental data at 80 °C with a stoichiometric feed with the three alkene feeds.

It turned out that the adsorption constant of ether was higher than that of methanol ($K_{eth}/K_{MeOH} = 2.4$), and therefore we made one further modeling to test if the assumptions made in the derivation of the rate equations were adequate. For this, we divided the numerator and denominator of eq 13 by K_{eth} instead of K_{MeOH} . Now the adsorption constant ratio K_{MeOH}/K_{eth} , which is the inverse of the ratio in the first modeling, appeared in the denominator. The ratio also remained

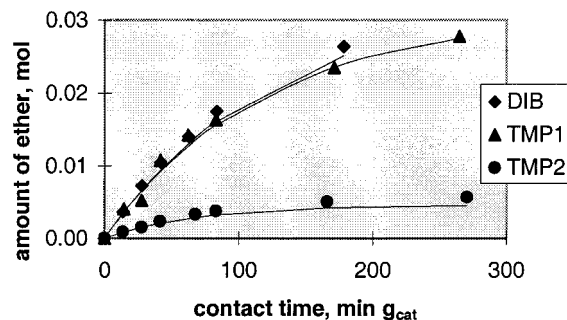


Figure 2. Amounts of ether measured at 80 °C (data points) and corresponding amounts estimated with the ER model (solid line).

in the numerator, but to ease the modeling, it was lumped with the rate constant k_i . The results are presented in Table 2 (rearranged ER model). Now we obtained a K_{MeOH}/K_{eth} ratio of approximately 1, which confirms that the adsorption constants of methanol and ether indeed are of the same order of magnitude. Thus, it is irrelevant in the derivation of the rate equations whether the equation is divided by K_{eth} or K_{MeOH} .

We also checked the validity of dropping out the first term of the denominator of eq 13. When this term was included in the modeling, the parameters showed high correlation and were not well identified. Thus, dropping of the first term of the denominator of eq 13 is crucial from the point of view of the calculation: without this term the parameters are much more easily identified.

LH-Type Model. The LH model included eight fitted parameters, i.e., in addition to the parameters included in ER model, and also the ratio K_{TMP}/K_{MeOH} . The larger number of parameters made it more difficult to model than the ER model. Furthermore, the parameters easily correlated with each other, which was not the case with the previous models.

The activation energy for the isomerization reaction was determined in the same way as that with the ER model, i.e., without the data from the isomer mixture experiments. However, this resulted in poor convergence of the parameters; the data had to be split, and each temperature was modeled separately. The activation energy of 103 kJ/mol was obtained for the isomerization reaction by regression analysis from the reaction rate constants, and this value was fixed for the fitting of the rest of the parameters. However, the parameters were not as accurately identified in the fit for the three experiments at 70 °C as they were at other temperatures. As seen in Figure 3, this led to a deviation from linearity compared with the rate constants at other temperatures, and as a result the error estimate for E_3 , 20 kJ/mol, was high relative to other error estimates. E_3 was also fitted by fixing the adsorption constant ratios and changing the fixed values. The results were

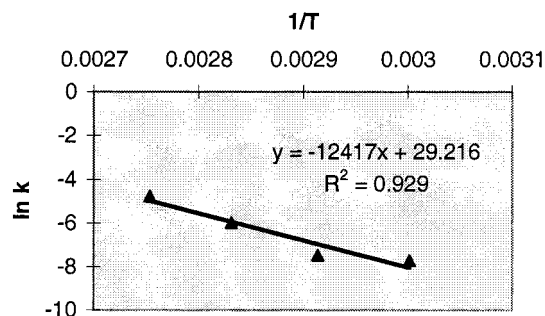


Figure 3. Determination of E_3 with the LH model.

close to our final values, but despite the large error estimate, the E_3 value obtained by the regression was considered to be the most accurate because none of the parameters were then fixed in the modeling.

After E_3 was fixed at a value of 103 kJ/mol, all of the remaining parameters could be modeled simultaneously with the whole data set of Table 1, which was not possible without fixing at least one of the parameters. Now, contrary to the respective fit with the ER model, the values of some parameters changed from the values estimated with the pure feed data: the reaction rate constants increased, and the $K_{\text{TMP}}/K_{\text{MeOH}}$ ratio decreased. This was assumed to be due to the high correlation of the parameters.

The fit was observed to be more dependent on the initial values of the parameters than in the ER model. In addition, the correlation between the parameters was high. In particular, the $K_{\text{TMP}}/K_{\text{MeOH}}$ ratio correlated with the reaction rate constants, and the reaction rate constants correlated with each other (correlation coefficient >0.97). On the basis of the statistics, this fitting of the LH model was thus the least reliable, even though the parameters converged quite well and the residual sum of squares was similar to those obtained with the other models.

To diminish the difficulties caused by the fixing of some parameters, we tried modeling the LH-type rate equations without the alkene adsorption term in the denominator of eqs 20 and 21; this is reasonable because, with $K_{\text{TMP}}/K_{\text{MeOH}}$ modeled to be relatively small (0.14), the adsorption of the alkenes is not very strong. In the numerator, the $K_{\text{TMP}}/K_{\text{MeOH}}$ ratio was lumped with the reaction rate constant and the number of fitted parameters was reduced to seven. Now the rate equations of etherification resemble the respective ER equations, but the denominator is squared.

This effect of removing the alkene adsorption term was first tested with the whole data set and then with the data of the isomer mixture experiments excluded. Results were similar in the two cases, which means that the isomerization reaction does not disturb the fit with the LH model when the adsorption term for the alkenes is not included in the rate equation.

Relative to the first modeling, with the alkene adsorption term included, the results changed somewhat, as presented in Table 2: the activation energies of the etherification reactions remained approximately the same, but the activation energy for the isomerization was increased by over 30 kJ/mol. The adsorption constant ratio $K_{\text{eth}}/K_{\text{MeOH}}$ was decreased slightly but was still 2.5. The correlation between the parameters was essentially weaker than that in the first LH modeling, and the correlation matrix resembled the corresponding matrix in the ER modeling. Thus, the system was

mathematically close to the ER model, and the fit was more reliable.

Comparison of the Kinetic Models. The fitted kinetic parameters of the different models are collected in Table 2. As can be seen, the values of all models are physically meaningful and they also agree well with the values presented in the literature for similar kinds of reaction systems. Our activation energies for the etherification were 80–94 kJ/mol, while earlier values were 82 kJ/mol for ETBE,¹¹ 84–92 kJ/mol for TAME,¹³ and 93–109 kJ/mol for THEE.¹⁹ Our activation energies for the isomerization reaction were 99–137 kJ/mol, and in similar kinds of systems, values of 91 kJ/mol for C_5 alkenes³² and 89–96 kJ/mol for C_6 alkenes^{19,21} have been obtained. This indicates that internal diffusion, which would lower the activation energies, is not important in our system. The same was found in our previous work.²²

The rate constants for the two etherification reactions are closely similar to those of all of the mechanisms, and they are approximately equal within experimental error. With other etherification reactions, it has been observed that the alkene isomer that is thermodynamically more stable is less reactive in etherification (e.g., C_5 's¹² and C_6 's¹⁹).

The estimated parameters indicate that more ether is adsorbed on the catalyst than methanol, and alkenes are adsorbed least. The ratio of the adsorption constants $K_{\text{eth}}/K_{\text{MeOH}}$ shows a similar trend with the ER and LH models: the adsorption constant of ether is over twice as large as that of methanol. It has been claimed³³ that alcohol should adsorb more easily than ether on ion-exchange resin beads, but this was not the case with the fibrous catalyst. Situations are somewhat different in an ion-exchange resin bead and on the surface of a fiber. Although the catalytically active sites are the same (sulfonic acid), the structures of the catalysts differ and the adsorbing species do not adsorb on the fiber in a similar way. Thus, what happens on a resin particle cannot simply be concluded to happen on a fibrous catalyst.

The different behaviors of ion-exchange resin and fiber may depend on the hydrophilic properties of the two catalysts. Both the polyethylene (fiber) and styrene-divinylbenzene (resin bead) matrixes are hydrophobic, but sulfonic acid, which is present in both matrixes, has hydrophilic properties. Some parts of the polyethylene matrix are amorphous and some parts crystalline, and it has been demonstrated that the grafting reaction occurs mainly in the amorphous region.³⁴ The grafted styrene is sulfonated, and the sulfonic acid sites are thus located solely in the amorphous region. Although the catalyst is heated during the sulfonation, and the crystalline parts become amorphous, this has no effect on the sulfonic acid distribution because only the grafted styrene is sulfonated. Thus, the parts of the polyethylene matrix that originally were crystalline remain hydrophobic, while the sulfonated parts have hydrophilic properties. In the resin matrix, in turn, no differences between various parts of the matrix should exist. Another difference between the fiber and the resin is how sulfonic acid is attached to the matrix: in the fiber the polyethylene is grafted with styrene and the grafts are sulfonated, but in the resin the styrene-divinylbenzene matrix itself is sulfonated. Because of this, the surface of the resin is likely to be more hydrophilic, but the fiber contains more hydrophobic

parts and fewer polar components such as ether can reach the fiber more easily than the more polar methanol. Thus, the ether adsorbs more readily on the fiber, and the ratio of the adsorption constants $K_{\text{eth}}/K_{\text{MeOH}}$ obtains a value greater than 1.

The concentrations of the reacting components near the active sites may be different in fiber and resin because of hydrophilic properties. However, once the components reach the active sites and reaction occurs, the mechanisms probably are the same, for the activation energies are similar to those reported in the literature for similar kinds of etherification reactions but with ion-exchange resins as catalysts.

The ratio of $K_{\text{TMP}}/K_{\text{MeOH}}$ appeared only in the LH model where it obtained a value of 0.14. This result can be compared with results for TAME in the literature: namely, a value of 3×10^{-8} has been reported for the adsorption constant ratio of isoamylenes and methanol on an ion-exchange resin.³³ The higher value for the fiber implies that the adsorption of alkenes is considerably easier on the surface of the fibrous catalyst than on the pores of the ion-exchange resin. Again, this result can be explained by the differences in the hydrophilic properties of the catalysts.

Figure 1 compares the fits of the different mechanisms. If the fit is perfect, the data points are located on the diagonal of the figure. The R^2 values of the mechanisms are almost the same. Thus, all mechanisms appear to represent the data equally well. Because the resulting parameters are also physically meaningful in each case, it is difficult to decide on the basis of the results which is the best model. The weakness of the ER model is the isomerization reaction: according to this model, the isomerization reaction occurs noncatalytically. However, the isomerization rate was greatly affected by the amount of methanol; e.g., the isomerization rate of TMP1 to TMP2 was 3 times as fast with a methanol-alkene molar ratio of 1 as with a molar ratio of 2 when the amount of alkene remained approximately constant. This indicates that the isomerization reaction is not totally independent of the catalyst and the rest of the reaction mixture. The LH model, for its part, was not easy to model as such, and the high correlation between the parameters indicates that the fit may not be the best possible. Modification of the LH model by omitting the alkene adsorption term improved the fit markedly.

As a matter of fact, the model may even change as a function of the reactant mole fractions, as stated by Tejero et al.³⁵ They concluded that when methanol was in excess in MTBE synthesis, the ER model described the system, and as the fraction of alkene was increased, the LH model began to predominate. In our system, the conversion profiles to ether and to isomer did not change as a function of the reactant mole fractions, which indicates that the mechanism would not change. According to our modeling, the ER and LH models where the adsorption of alkenes is assumed to be small gave equal fits.

Conclusions

Etherification of 2,4,4-trimethyl-1-pentene and 2,4,4-trimethyl-2-pentene with methanol was catalyzed with a fibrous Smopex-101 catalyst. ER- and LH-type kinetic models were derived for the reaction and compared.

The difference between the models was not very striking, probably because of the narrow temperature

range. Although the temperature range was narrow, it was also the commercially interesting range, and thus it was justified to concentrate the studies on these conditions. The models represented the data equally well with physically meaningful parameters, but the ER and LH models where the alkene adsorption of alkenes is assumed to be small could be judged to best describe the data.

The activation energy estimated for the etherification of 2,4,4-trimethyl-1-pentene was 86–94 kJ/mol, for the etherification of 2,4,4-trimethyl-2-pentene 80–90 kJ/mol, and for the isomerization of 2,4,4-trimethyl-1-pentene to 2,4,4-trimethyl-2-pentene 99–137 kJ/mol. The estimated adsorption constants indicate that more ether than methanol is adsorbed on the catalyst. This can be explained by the hydrophobic properties of the fibrous Smopex catalyst.

Acknowledgment

We are grateful to Fortum Oil and Gas Oy for financial support and for providing the ether. Special thanks go to Ms. Riitta Saarinen for experimental assistance.

Notation

- a_i = activity of component i
- E_i = activation energy, kJ/mol
- k_i = reaction rate constant, mol/(kg s)
- K_i = adsorption constant of component i (i abbreviation)
- K_i = equilibrium constant of reaction i (i numeral)
- P = fitted parameter
- r_i = formation rate of component i , mol/(kg s)
- R = 8.314 J/(mol K)
- T = temperature, K or °C
- Θ_i = surface coverage of component i

Abbreviations

- eth = ether
- MeOH = methanol
- S = active surface site of the catalyst
- TMP1 = 2,4,4-trimethyl-1-pentene
- TMP2 = 2,4,4-trimethyl-2-pentene

Literature Cited

- (1) Executive order D-5-99 by the Governor of the State of California, Mar 25, 1999.
- (2) Sloan, H. D.; Birkhoff, R.; Gilbert, M. F.; Pyh lahti, A.; Nurminen, L. Isooctane Production from C₄'s as an Alternative to MTBE. NPRA 2000 Annual meeting (AM-00-34), Mar 26-28, 2000, San Antonio, TX.
- (3) Process Converts "Stranded" MTBE Units to Iso-octane. *Eur. Chem. News* **2000**, 72 (No. 1893), 35.
- (4) SP Isooctane Units Licensed. *Eur. Chem. News* **2000**, 72 (No. 1894), 39.
- (5) Di Girolamo, M.; Lami, M.; Marchionna, M.; Pescarollo, E.; Tagliabue, L.; Ancillotti, F. Liquid-Phase Etherification/Dimerization of Isobutene over Sulfonic Acid Resins. *Ind. Eng. Chem. Res.* **1997**, 36, 4452-4458.
- (6) Karinen, R. S.; Krause, A. O. I. Reactivity of Some C₃-Olefins in Etherification with Methanol. *Appl. Catal. A* **1999**, 188, 249-256.
- (7) Papachristos, M. J.; Swithenbank, J.; Priestman, G. H.; Stournas, S.; Polysis, P.; Lois, E. The Effect of the Molecular Structure of Antiknock Additives on Engine Performance. *J. Inst. Energy* **1991**, 64, 113-123.
- (8) Kivi, J. (Fortum Oil and Gas Oy). Personal communication, Dec 1, 2000.
- (9) Piel, W. J. Diversify Future Fuel Needs with Ethers. *Fuel Reformulation* **1994**, 4 (No. 2), 28-33.

- (10) Al-Jarallah, A. M.; Siddiqui, M. A. B.; Lee, A. K. K. Kinetics of Methyl Tertiary Butyl Ether Synthesis Catalysed by Ion Exchange Resin. *Can. J. Chem. Eng.* **1988**, *66*, 802–807.
- (11) François, O.; Thyron, F. C. Kinetics and Mechanism of Ethyl *tert*-Butyl Ether Liquid-phase Synthesis. *Chem. Eng. Process.* **1991**, *30*, 141–149.
- (12) Rihko, L. K.; Kiviranta-Pääkkönen, P. K.; Krause, A. O. I. Kinetic Model for the Etherification of Isoamylenes with Methanol. *Ind. Eng. Chem. Res.* **1997**, *36*, 614–621.
- (13) Piccoli, R. L.; Lovisi, H. R. Kinetic and Thermodynamic Study of the Liquid-phase Etherification of Isoamylenes with Methanol. *Ind. Eng. Chem. Res.* **1995**, *34*, 510–515.
- (14) Fité, C.; Iborra, M.; Tejero, J.; Izquierdo, J. F.; Cunill, F. Kinetics of the Liquid-Phase Synthesis of Ethyl *tert*-Butyl Ether. *Ind. Eng. Chem. Res.* **1994**, *33*, 581–591.
- (15) Jayadeokar, S. S.; Sharma, M. M. Simultaneous Hydration and Etherification of Isoamylenes Using Sub-azeotropic Ethanol. *React. Polym.* **1993**, *19*, 169–179.
- (16) Iborra, M.; Izquierdo, J. F.; Cunill, F.; Tejero, J. Application of the Response Surface Methodology to the Kinetic Study of the Gas-Phase Addition of Ethanol to Isobutene on a Sulfonated Styrene-Divinylbenzene Resin. *Ind. Eng. Chem. Res.* **1992**, *31*, 1840–1848.
- (17) Oost, C.; Hoffmann, U. The Synthesis of Tertiary Amyl Methyl Ether (TAME): Microkinetics of the Reactions. *Chem. Eng. Sci.* **1996**, *51*, 329–340.
- (18) Linnekoski, J. A.; Krause, A. O. I.; Rihko, L. K. Kinetics of the Heterogeneously Catalyzed Formation of *tert*-Amyl Ethyl Ether. *Ind. Eng. Chem. Res.* **1997**, *36*, 310–316.
- (19) Zhang, T.; Datta, R. Ethers from Ethanol. 4. Kinetics of the Liquid-Phase Synthesis of Two *tert*-Hexyl Ethyl Ethers. *Ind. Eng. Chem. Res.* **1995**, *34*, 2247–2257.
- (20) Pescarollo, E.; Trotta, R.; Sarathy, P. R. Etherify Light Gasolines. *Hydrocarbon Process.* **1993**, *72* (No. 2), 53–60.
- (21) Zhang, T.; Datta, R. Ethers from ethanol. 5. Equilibria and Kinetics of the Coupled Reaction Network of 3-Methyl-3-Ethoxy-pentane Synthesis. *Chem. Eng. Sci.* **1996**, *51*, 649–661.
- (22) Karinen, R. S.; Krause, A. O. I.; Ekman, K.; Sundell, M.; Peltonen, R. Etherification over a Novel Acid Catalyst. *Stud. Surf. Sci. Catal.* **2000**, *130*, 3411–3416.
- (23) Cunill, F.; Vila, M.; Izquierdo, J. F.; Iborra, M.; Tejero, J. Effect of Water Presence on Methyl *tert*-Butyl Ether and Ethyl *tert*-Butyl Ether Liquid-Phase Syntheses. *Ind. Eng. Chem. Res.* **1993**, *32*, 564–569.
- (24) Linnekoski, J. A.; Krause, A. O. I.; Struckmann, L. K. Etherification and Hydration of Isoamylenes with Ion Exchange Resin. *Appl. Catal. A* **1998**, *170*, 117–126.
- (25) Karinen, R. S.; Lylykangas, M. S.; Krause, A. O. I. Reaction Equilibrium of the Isomerisation of 2,4,4-Trimethylpentenes. *Ind. Eng. Chem. Res.* **2001**, *40*, 1011–1015.
- (26) Rihko-Struckmann, L. K.; Karinen, R. S.; Krause, A. O. I.; Aittamaa, J. R. The Production of a Novel Oxygenated Gasoline Component. Manuscript in preparation.
- (27) Agarwal, A. K.; Brisk, M. L. Sequential Experimental Design for Precise Parameter Estimation. 1. Use of Reparametrization. *Ind. Eng. Chem. Process Des. Dev.* **1985**, *24*, 203–207.
- (28) Helfferich, F. *Ion Exchange*; McGraw-Hill Book Co.: New York, 1962; p 511.
- (29) Sola, L.; Pericàs, M. A.; Cunill, F.; Iborra, M. Reaction Calorimetry Study of the Liquid-phase Synthesis of *tert*-Butyl Methyl Ether. *Ind. Eng. Chem. Res.* **1994**, *33*, 2578–2583.
- (30) Aittamaa, J.; Keskinen, K. I. Kinfitec, Laboratory of Chemical Engineering, Helsinki University of Technology, 2000.
- (31) Fredenslund, A.; Gmehling, A.; Rasmussen, P. *Vapour-Liquid Equilibria Using Unifac*; Elsevier: New York, 1977; p 380.
- (32) Linnekoski, J. A.; Kiviranta-Pääkkönen, P.; Krause, A. O. I.; Rihko-Struckmann, L. K. Simultaneous Isomerization and Etherification of Isoamylenes. *Ind. Eng. Chem. Res.* **1999**, *38*, 4563–4570.
- (33) Rihko, L. K.; Krause, A. O. I. Kinetics of Heterogeneously Catalysed *tert*-Amyl Methyl Ether Reactions in the Liquid Phase. *Ind. Eng. Chem. Res.* **1995**, *34*, 1172–1180.
- (34) Hietala, S.; Holmberg, S.; Karjalainen, M.; Näsman, J.; Paronen, M.; Serimaa, R.; Sundholm, F.; Vahvaselkä, S. Structural Investigations of Radiation Grafted and Sulfonated Poly(vinylidene fluoride), PVDF, Membranes. *J. Mater. Chem.* **1997**, *7*, 721–726.
- (35) Tejero, J.; Cunill, F.; Izquierdo, J. F.; Iborra, M.; Fité, C.; Parra, D. Scope and Limitations of Mechanistic Inferences from Kinetic Studies on Acidic Macroporous Resins. The MTBE Liquid-Phase Synthesis Case. *Appl. Catal.* **1996**, *134*, 21–36.

Received for review May 4, 2001

Revised manuscript received September 25, 2001

Accepted September 30, 2001

IE010409C